FE3O4 DECORATED TIO2 NANO TUBE PHOTO CATALYST SEMICONDUCTOR

M.DEEPA[1],M.MOHANAPRIYA [2],R.SHANMUGAPRIYA[3],M.MAHALAKSHMI[4]

A b s t r a c t

Fe_3O_4-TiO_2 nanocomposite photocatalyst with different weight percentage (5, 10, and 15 wt %) of Fe_3O_4 loaded On TiO_2 were successfully synthesized by co-precipitation method for removal of methylene blue dye under direct sunlight. The characterization of the as prepared product was done with scanning electronic microscopy (FE-SEM), X-ray diffraction (XRD), and Diffuse reflectance spectra (DRS). The photocatalytic degradation of methylene blue was used as modal reaction to evaluate the photocatalytic activity of Fe_3O_4@TiO_2 nanoparticles under visible light irradiation . The influence of doping amount of Fe_3O_4 (5, 10, 15 wt%) on photocatalytic activity of TiO_2 was investigated. Broadened absorption spectra has describe that the size of Fe_3O_4@TiO_2 particle decreased with increased absorption intensity. The doping amount remarkably affects the activity of the catalyst, and the optimum efficiency occurs at about the doping amount of 10 wt%. The catalytic activity of TiO_2 increased for methylene blue (MB).

Background of Environmental pollution

Environmental pollution, such as contaminated water or/and polluted air, has become a global issue threatening the health of mankind. Typical polluting sources are toxic organic molecules or exhaust gas compounds which are released from household waste, livestock waste, and local industries. This extensive disposal of textile and other industrial waste water that contains organic dyes creates a severe contamination throughout the world. About 1 to 20% of the total dyes produced globally are lost during dyeing and other processes. These dyes are released into water as such [1-3]. These organic dyes weathered through oxidation; hydrolysis and other chemical reactions taking place in the wastewater phase can produce toxic metabolites [4, 5]. These products produce unfavorable effects on human and animal health, which requires a suitable treatment of wastewater for environmental contamination prevention [6]. Different solutions for depollution have already been proposed: air scrubbing, adsorption, activated carbon, etc., but some of them only convert the pollutant from one phase to another one and then require additional processes to eliminate toxic compounds.

The photo-catalytic splitting of water on TiO_2 electrodes involved in Heterogeneous photo-catalysis [7]. This technique can be envisaged as one of the most promising Advanced Oxidation Process (AOPs) because of its specific advantages, such as bland reaction conditions, the possibility of using molecular oxygen as oxidant species, the total mineralization of pollutants into substances nontoxic to the environment. Heterogeneous photocatalysis is based on the interaction between semiconductor materials and light. By considering that we can get 'free' light from the sun, the idea of using solar light energy as resource to clean up the environment is an ideal and extremely promising approach. Sun light, with wavelengths ranging from 200 to 1000 nm, is a clean and renewable energy source that is readily available. Before reaching the Earth's surface, a part of the solar energy is absorbed by the stratosphere, ozonosphere, and other atmospheric layers. the photochemical processes such as synthesis of vitamin D composed of UV at three regions are A (315 – 400 nm), B (280 – 315 nm) and C(100 – 280 nm), occur.

Fig.1. solar spectrum.

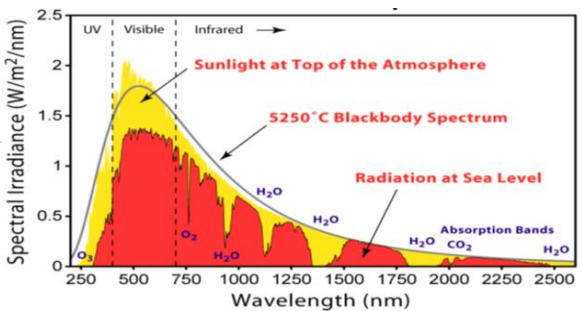

1.2 Principles of semiconductor photocatalysis

The most commonly used photocatalysts are semiconductor materials (most of them metal oxides) which, unlike metals, possess a void energy region (band-energy structure), where no energy levels are available (Fig. 2). The void region which extends from the top of the filled valence band to the bottom of the vacant conduction band is called band gap, Eg.

Activation of a semiconductor photocatalyst is achieved through the absorption of a photon of ultra-band gap energy, which results in the promotion of an electron from the valence band into the conduction band, e- CB, and in the concomitant generation of a hole in the valence band, h+ VB. The reaction of either the photopromoted electron with a reducible adsorbed substrate (usually oxygen in aerated system) and/or the hole with an oxidizable adsorbed species can subsequently occur. The probability and the rate of such charge transfer processes depend on the position of the conduction and valence band edges and on the redox potentials of the adsorbed species. At the same time the photogenerated electron in the conduction band should be negative enough to reduce adsorbed O_2 to superoxide radical anion [9].

Fig. 2 Simplified scheme of semiconductor activation.

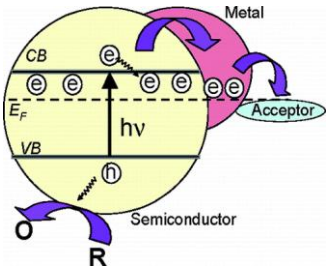

The probability and the rate of such charge transfer processes depend on the position of the conduction and valence band edges and on the redox potentials of the adsorbed species. semiconductor is involving in the photodecomposition or complete mineralization of organic pollutants, it should be capable to generate a valence band hole with a redox potential that is positive enough to oxidise the organic pollutant. At the same time the photogenerated electron in the conduction band should be negative enough to reduce adsorbed O_2 to superoxide radical anion [9].

1.3 TiO_2 as photocatalyst

As for any common catalytic material, which is not consumed during the course of a chemical reaction, a photocatalyst must be stable and not prone to decompose due to long exposure to light. pH is essential in water suspensions are used,. As a general rule, a good photocatalyst must be photoactive [10].

- Able to absorb visible and/or near UV light
- Biologically and chemically inert
- Photostable (i.e. not liable to photoanodic corrosion)
- Inexpensive and non-toxic.

In many cases, the semiconductor risks to gain in oxidative decomposition by the photogenerated holes. Generally, only n-type semiconductor oxides are stable towards photoanodic corrosion,. CdS is an example of a highly active semiconductor which can be activated using visible light (thus, sunlight could be used), but, as usually occurs for visible light absorbing semiconductors, it is subject to photoanodic corrosion and this feature makes it unacceptable as a photocatalyst for water purification.

Among different semiconductor photocatalysts, TiO_2 appears as the most active and most suitable one for a wide variety of energy and environmental applications. In fact, TiO_2 has a high strong oxidizing power; moreover, it is biologically, universal applicability and chemically inert, cost effectiveness, and long-term stability against photo-corrosion. Finally the location of the bottom of conduction band is suitable for using this material for the photocatalytic production of hydrogen from water, which has received extensive attention in the last decade for its potential application in the field of solar energy harvesting, conversion and storage [11, 12]. However, the photocatalytic

efficiency of TiO_2 using natural sunlight is currently very low. Several factors are of relevance, but two are more important: the fast recombination of photogenerated electron-hole pairs and the limited optical response only to UV light. Thus, to inhibit the recombination of photogenerated electron-hole pairs and to extend the optical absorption to visible light region is two key ways to improve the photocatalytic activity of TiO_2 under solar irradiation. In order to extend the optical absorption of TiO_2 to the visible light region, various attempts have been made to modify TiO_2 [14] including surface deposition of noble metallic nanoparticles, Photosensitization with organic dyes, polymers, and semiconductors, doping with cations and/or anions, and surface reduction treatment. Recently, the nanocomposites of TiO_2 and noble metallic nanoparticles have been intensively investigated because they can enhance the photocatalytic activity primarily by extending the optical absorption to the visible light region and increasing the number of photoexcited electrons due to the enhanced near-field amplitude [15-19].

The most common approach to sort out the problems associated with TiO_2 nanomaterials is the surface modification of TiO_2 by adopting few techniques, among which, the noble metal (Au, Ag, Pt etc) doping is found to be attractive. In this routes employed for sensitizing TiO_2 and have proved in significantly enhancing the photoactivity of TiO_2. The underlying mechanism being that the Fermi level of the metal is lower than TiO_2 and hence there can be an electron transfer from the conduction band of the semiconductor to the metal [26]. This consequently leads to significant reduction in the recombination of photo generated electrons and holes which is reflected in enhanced photocatalytic activity. However, the amount of noble metal loaded is crucial as excess of noble metal can lead to a decrease in photocatalytic activity mainly because it may hamper the photon absorption of TiO_2 and block its active sites. Moreover, at higher loadings, the noble metal may itself act as a recombination centre for photo generated electrons and holes further affecting the efficiency eventhough very recently High surface area Ag-TiO2 nanotubes for photocatalytic degradation of ceftiofur sodium. The TiO2 NTs exhibited better photocatalytic activity than TiO2 NPs due to their very high specific surface area and good crystallinity as well as the surface deposited Ag NPs significantly increased their photocatalytic degradation rate, owing to the plasmonic Ag NPs as well as due to the effective charge separation (electron–hole separation) at the Ag/TiO2 interface [27].

During the past few decades, magnetic nanoparticles with peculiar size and structure have attracted wide attention because of their unique physical and chemical properties [28, 29]. Of all magnetic materials, magnetite (Fe_3O_4) is the most important and most widely used one in many fields. When prepared into well-defined nanoscale structures, Fe_3O_4 may be practically or potentially applied in a wide range of fields, such as biomolecular separation, [30] chemical sensor, [31] energy storage, [32] catalysis, [33-35] microwave absorption, [36] and environmental remediation [37-41]. Generally speaking, Fe_3O_4 nanoparticles could be prepared with different methods including co-precipitation of Fe^{2+} and $Fe^{3+,}$ thermal decomposition, microemulsion, and hydrothermal and solvothermal [42,43]. Of all these methods, co-precipitation is a preferred choice for most researchers because the reaction could be performed under a mild condition by using water as solvent. Moreover, the magnetic separation provides a very convenient approach for removing and recycling magnetic particles/composites by applying an appropriate magnetic field. This approach may prevent the agglomeration of the catalyst particles during recovery and can

increase the durability of the catalysts. Catalysts have been immobilized on various magnetic supports, including polymers, [44] carbon, [45] and silica, [46] and other nanocomposites combining mesoporous materials with a high surface area and well-defined pore size with magnetic nanoparticles. [47] Unfortunately, research has been carried out by immobilizing TiO_2 onto various magnetic supports, such as magnetite, [48] ferrite, [49] barium ferrite, [50] and Fe_3O_4@SiO_2 particles [51]. These magnetic photocatalysts can not only be recovered but also fluidized by applying an external magnetic field. However, most of the research group works in this area have focused on different nanostructures and the resulting magnetic photocatalysts are not considerable photo catalytic activity. From this viewpoint, we propose a flexible process for fabricating different weight percentage (5, 10, and 15 wt %) of magnetic Fe_3O_4 core-shell NPs by using co-precipitating method. This route is useful to obtain interesting and controllable attention with TiO_2 nonporous outside with using methylene blue dye. To the best of our knowledge, few researchers have been approached in this way eventhough no one can report optimization of magnetic TiO_2 nanoporous decorated by Fe_3O_4 core-shell nanoparticles for photocatalyst. This aims at enhancing the photocatalytic efficiency of TiO_2 as much as possible so as to meet the widespread applications as well as encourage further research in this area.

Materials & Methods

Chemical reagents such as high pure Titanium isopropoxide were purchased from Alfa aeser. Ferrous sulphate hepta hydrate ($FeSO_4$•$7H_2O$) was received from Merck. Ferric chloride ($FeCl_3$) was procured from SigmaAldrich and Tri sodium citrate was obtained from Merck and all the other chemicals used in this work were of analytical grade. Unless otherwise mentioned, double distilled water was used for the preparation of aqueous solutions and washings.

Preparation of TiO_2 nanoparticles

In the present study, the TiO_2 nanoparticles were prepared via the sol–gel method.. Titanium isopropoxide was used to prepare transparent TiO_2 sol at room temperature as follows. The Titanium isopropoxide was dissolved in ethanol and stirred for half an hour to get a precursor solution. A mixture of distilled water, glacial acetic acid, and ethanol was then dropped into the precursor solution at a speed of one drop per second under vigorous stirring. After that, the solution was continuously stirred for 1h to achieve a transparent yellow TiO_2 sol. The sol was dried at 110 °C for 3h and then the obtained gel was heat treated at 400 °C for 2h.

. Preparation of Fe_3O_4 nanoparticles

An iron oxide dispersion was prepared using an established method [60]. Briefly, FeCl3 (3.5035 g, 0.0216 mol) and $FeSO_4 \cdot 7H_2O$ (3.003 g, 0.0108 mol) in the molar ratio of 2:1 were dissolved in 100 mL of deoxygenated water using nitrogen gas at 85°C under vigorous mechanical stirring in a nitrogen atmosphere. Then, 7.5 mL of ammonium hydroxide was quickly injected into the reaction mixture. This resulted in immediate formation of a black precipitate of magnetic NPs. The magnetite dispersion was stirred for 30 min and then cooled to room temperature. The black precipitate was washed several times with deionized water and twice with 0.02 mol/L sodium chloride by magnetic decantation.

. Preparation of modified Fe_3O_4 nanoparticles

The modified Fe_3O_4 nanoparticles were synthesis following reported procedure

[61]. Briefly, The surface modification of Fe_3O_4 nanoparticles was carried out by the reaction of the nanoparticles with sodium citrate. Fe_3O_4 nanoparticles (4g) and 200 mL sodium citrate 0.5M were mixed together in a 250 mL beaker. The mixture was kept under ultrasonic irradiation for 30 min to reduce the aggregation of modified nanoparticles, and then stirred for 12h at a temperature of 110 °C under Argon protection. The precipitate was collected by magneticfield separation and was washed with acetone several times.

Preparation of Fe_3O_4@TiO_2 core-shell nanocomposite

To prepare the core–shell particles of Fe_3O_4@TiO_2, the modified magnetic coreparticles were initially dispersed in 100 mL deionised water and kept under ultrasonic irradiation for 30 min to obtain a stable ferro fluid. This was followed by the addition of TiO_2 nanoparticles. Molar ratio of Fe_3O_4 to TiO_2 was kept to 1:10. The mixture was then stirred for 30min and dried at 110 °C under vacuum, so that a gray nanopowder of Fe_3O_4@TiO_2 was finally formed. The prepared samples were then characterized by XRD, SEM, and DRS.

Characterization Studies

Absorprion spectra of different wt% of Fe_3O_4@TiO_2 catalyst were recorded using UV-vis spectrophotometer (UV-2550, Shimadzu). Diffuse reflectance spectra (DRS) of different nanocomposite of Fe_3O_4@TiO_2 and pristine TiO_2 nanoparticles powder were taken using ISR-2200 DRS accessory of UV-vis spectrophotometer (UV-2550, Shimadzu). Powder XRD analyses of the samples were recorded on Scintag-XDS-2000 spectrometer with Cu Kα a radiation with applied voltage of 40 kV and current of 30 mA and Scanning Electronic Microscopy (SEM) images were aquired in TESCAN VEGA3 Scanning Electron Microscope.

. Photocatalytic activity measurement

Photocatalytic activities of Fe_3O_4@TiO_2 core-shells were evaluated by the degradation of methylene blue dye under sunlight irradiation with a cut off filter measuring of 395 nm. The reaction cell was placed in a sealed black box with an opening on the top, and the cutoff filter was placed to provide visible-light irradiation. In a typical process, 0.05 g of photocatalyst was added into 100 mL of methylene blue dye with a concentration of 1.05g L^{-1}. After being dispersed in an ultrasonic bath for 5 min, the solution was stirred for 30 min in the dark to reach the adsorption/desorption equilibrium between the catalyst and the selected methylene blue dye. Then, the suspension was exposed to the visible light irradiation [62]. The samples were collected at given time intervals and the dye concentration was measured by using UV-vis spectroscopy. The experiment was repeated thrice to study the regeneration and reusability of the photocatalyst.

Results & Discussion

.1. HR-SEM Investigation of Fe_3O_4@TiO_2 nanocomposite

The magnetic nature of the prepared Fe_3O_4 and Fe_3O_4 @TiO_2 nanocomposites were tested with external magnets. When the external magnets were placed on the walls of the glass vial containing the dispersions of the Fe_3O_4 or Fe_3O_4@TiO_2, all the particles were attracted by the external magnetic field towards the walls of the vial containing the magnetic nature of the samples (Fig.3).

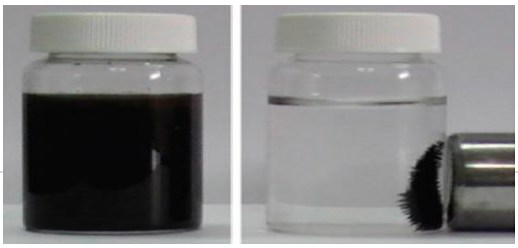

Fig.3. The Photog

raphical image of magnetic nature of prepared Fe_3O_4 @TiO_2 Core-shell nanocomposites.

The SEM images of the as-synthesized of Fe_3O_4@TiO_2 nanocomposite with different weight percentage Fe_3O_4 are shown in Fig.4. The SEM image of the Fe_3O_4 nanoparticles was found from the SEM micrograph (Fig.4). It can be seen that a uniform shell of TiO_2 with a nano-scale thickness is coated on the modified Fe_3O_4 surface to form a core–shell structure. The spherical shape of the cores will change in to ellipsoid with an average size of 5- 50 µm and the average thickness of the shell is 5µm (Fig.4a). The dark and bright regions corresponding to the Fe_3O_4 and the shell respectively. This phenomenon can be due to their different electron-absorbing abilities; therefore the electron binding ability of Fe_3O_4 is higher than that of non-magnetic TiO_2.

Fig.4 The SEM images of the as-prepared Fe_3O_4@TiO_2 (5 wt%) (a) and Fe_3O_4@TiO_2 (b) nanocomposite.

IV.2. Diffuse Reflectance Spectral (DRS) Characterization Studies

The UV-vis DRS spectra of pristine TiO_2 NPs, bare Fe_3O_4 NPs and Fe_3O_4@TiO_2 core-shell nanoparticles with different wt% of (5, 10, 15 wt%) Fe_3O_4 are shown in Fig.5. The absorption edge of these samples shows a remarkable shift to the visible range and the intensity increases with the increase of the amount. This is mainly due to that Fe^{3+} inserts into the structure of titanium dioxide, occupies some of the Ti^{4+} lattice sites because of diffusion and transfer of the ions, and forms impurity interim levels between valence and conduction bands in TiO_2. The impurity interim levels form impurity energy band, which overlaps with the TiO_2 conduction band as the amount of impurity increases [63]. However, it was observed that the pristine TiO_2 shows its characteristic absorption peak positioned at 400 nm which is intermediate between purely anatase (387 nm) and rutile (400 nm) indicative that both the phases are present in the sample. However, The DRS of Fe_3O_4@TiO_2 (5 wt%), Fe_3O_4@TiO_2 (10 wt%) and Fe_3O_4@TiO_2 (15 wt%) show broad band between 400 and 600 nm, in the visible region. Moreover, all the samples show the characteristic absorption peak of pristine nanoparticles of 400 nm, which indicates that there is no chemical transformation took place in pristine TiO_2 nanoparticle, which is an essential requirement for obtaining good performance in photocatalytic dye degradation of organic pollutants.

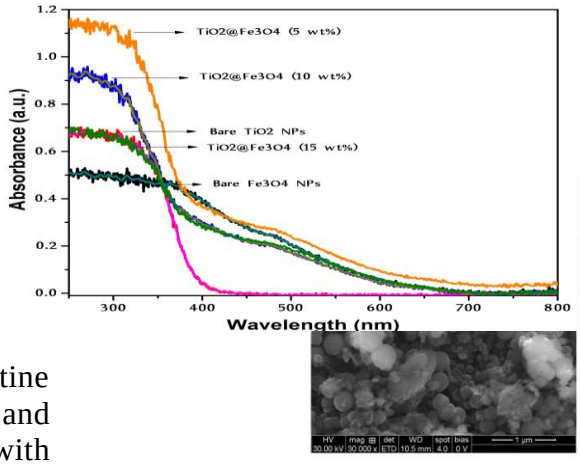

Fig.5. Diffuse reflectance spectra of Fe_3O_4@TiO_2 core-shell nanoparticles

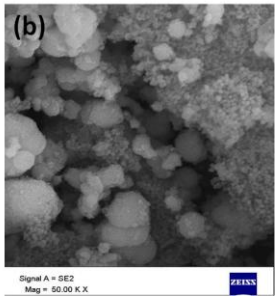

IV.3. X-ray diffraction analysis of TiO_2 and Fe_3O_4@TiO_2 core-shell nanoparticles

The X-ray diffraction patterns of the prepared Fe_3O_4 NPs and TiO_2 coated Fe_3O_4 nanoparticles are shown in Fig.6. It can be seen that TiO_2 nanoparticles are made of mixture of anatase and rutile phases when the doping amount of Fe_3O_4 is lower than 5wt%. In the range of 0.0 – 5 wt% , the

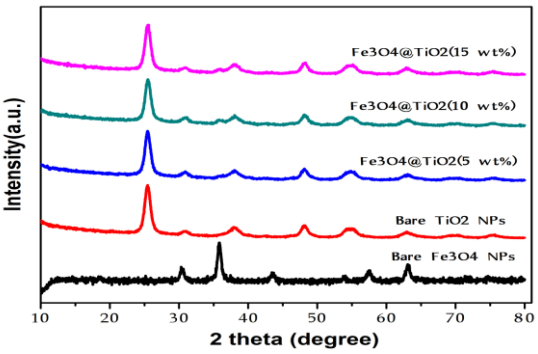

percentage of rutile phase increased with increases of the doping amount of Fe_3O_4. These results reveal that the doping amount of Fe_3O_4 controls the crystals structure of TiO_2 from anatase to rutile phase. The diffraction peaks are remarkably broadend. There are some factors affecting the diffraction peaks, such as the grain size, the defect of the crystal and so on. The observed peaks of prepared Fe_3O_4 in the XRD pattern can be indexed to the face-centered cubic phase of Fe_3O_4 (JCPDS No. 19-629). No impurity peaks are observed, which indicate that the product is pure Fe_3O_4 phase. The diffraction peaks at 2θ values of 30.3°, 36.0°, 43.3°, 57.4°, and 63.1° can be attributed respectively to the (2 2 0), (3 3 1), (4 0 0), (4 2 2) and (5 1 1) diffraction planes of the face-centered cubic phase of Fe_3O_4 (JCPDS No. 19-629) and. The XRD patterns of bare TiO_2 crystal show that diffraction peaks at 2θ values 25.3°, 38.0°, 48.1°, 54.8° and 62.8° are indexed as (101), (004), (200), (105), (211) plane of the anatase phase, whereas the peaks at 30.7° and 62.8° can be indexed as (110) and (111) planes of rutile phase. It is clear that the TiO_2 nanoparticles have the mixture of anatase and rutile phases [64]. The characteristic peak of the Fe_3O_4 are not observed in the studied doping range of Fe_3O_4@TiO_2. One of the reason may be the homogeneous dispersion of Fe_3O_4 in the TiO_2 lattice because similar ion radii of Fe^{3+} and Ti^{4+}, and other amount of doped Fe^{3+} in Fe_3O_4 is so low, that cannot be detected by XRD and weak diffraction peak of Fe_3O_4 are shielded by the broadened diffraction peak of TiO_2 with loaded Fe_3O_4. The XRD pattern of prepared Fe_3O_4 @TiO_2 also confirms that there are no other impurities present in the prepared samples. Besides, the 2θ values at which the major peaks appeared are found to be almost similar in both the pristine TiO_2 NPs and Fe_3O_4@TiO_2 core-shell nanoparticles.

Fig.6. XRD patterns of different wt% of Fe_3O_4@ TiO_2 nanocomposites.

IV.4. Photocatalytic degradation of methylene blue (MB)

The photodegradation of methylene blue (MB) was monitored by recording the absorption spectra with respect to time of irradiation and their corresponding degradation profiles are shown in Fig.7 (a-d) and Fig.8, where C_0 and C_t are the initial concentration and the MB dye concentration at irradiation time 't' min, respectively. Under direct sunlight irradiation bare TiO_2 degrades 75% of MB whereas 5 wt% of Fe_3O_4@TiO_2, 10 wt% of Fe_3O_4@TiO_2 and 15 wt% of Fe_3O_4@TiO_2 degrade 89%, 97% and 93% of MB respectively. It can be found that the photocatalytic activity initially increases with increasing amount of Fe_3O_4, reaches a maximum activity at about the 10 wt% and then decreases with further increasing of the doping amount of Fe_3O_4 on TiO_2. The photocatalytic activity is lower than that of bare TiO_2 when the doping amount increases to 15wt%. These results indicate that the photocatalytic activity of TiO_2 can be improved by doping an appropriate amount of Fe_3O_4 into TiO_2. The photocatalytic activitry of TiO_2 is improved most effectively when the doping amount is 10wt%, and the decolourization efficiency reaches 97% at a reaction time of 60 min, which showed a 22% increase as compared to bare TiO_2 with a decolourization efficiency of 75%. A similar system

observation was reported by Yan et al. [65]. To summarize the experimental results above, the main factors affecting the photocatalytic condition in our experimental condition may be the crystal and electron structures. These results consist with the study of Gao et al. [66], This study indicated that the separation between photo-generated electron and hole in the anatase crystal could be accelerated effectively when a thin layer of rutile crystal grows on the surface of anatase crystal and this may improve the photocatalytic activity. Hence, the photocatalytic activity of optimal when the doping amount of Fe_3O_4 is 10wt%.

Choi et al [67] considered that the transition from Fe^{3+} to Fe^{2+} corresponding to the transition from d^5 to d^6 , and Fe^{2+} relatively unstable due to the loss of exchange energy and tend to return to the Fe^{3+} , resulting in the release of the trapped electron becoming easy. However the energy level leis close to Ti^{3+}/Ti^{4+} level. As a consequence of this time the trapped electron Fe^{2+} can easily transferred to the near surficial Ti^{4+} and combine with oxygen molecule adsorbed on the surface to O_2^- and finally $^{\cdot}OH$, so the number of active group increases and photocatalytic activity also improved correspondingly. Furthermore, H_2O_2 may be produced in the catalytic reaction on TiO_2. From the Fenton reactive mechanism, the coexistence of Fe^{2+} and H_2O_2 in the acidic condition may produce $^{\cdot}OH$, which has strong oxidising power. Hence, it can be interfering the reaction. Considering that the above fact the vacancy introduced in the crystal lattice by Fe^{3+} make surface charges unbalanced. To keep the electron neutrality, the TiO_2 should be absorb more OH^- ions**,** which may react with photogenarated hole h^+ and form active $^{\cdot}OH$, and hence promote the photocatalytic efficiency. Therefore, the concentration of hole carrier may increase under visible light irradiation with increasing doping amount of $Fe_3O_{4@}TiO_2$ NPs.

The kinetic linear plots of photocatalytic degradation of methylene blue

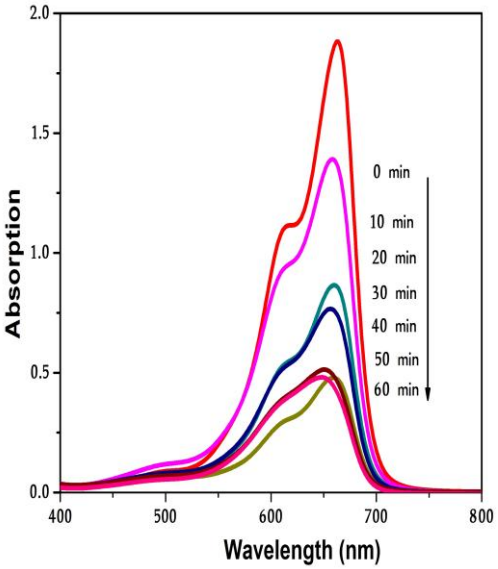

(MB) dye with TiO_2, 5% $Fe_3O_4@TiO_2$, 10% $Fe_3O_4@TiO_2$ and 15% $Fe_3O_4@TiO_2$ core-shell nanocomposites are shown in Figure.9. Usually the photocatalytic degradation of organic dyes by semiconductor under light irradiation generally involves the excitation of the semiconductor to form photogenerated (e–….h+) pairs and the subsequent chemical reactions with the surrounding media after the photogenerated holes move to the particle surface and react with organic dye molecules to form CO_2 and H_2O [68, 69]. The other possible mechanism is based on the excitation of dye in which the dye acts as a sensitizer under visible light as well as injects excited electrons to an electron acceptor to become a cationic dye radical (dye*+), followed by self - degradation of dye molecules [70].

Fig.7a The time dependent absorption spectra of MB recorded in the presence of bare TiO_2 nanoparticles under sunlight irradiation at different times. [Catalyst] = 1.05g/0.5L and [MB] = 1.6×10^{-5} M.

M.

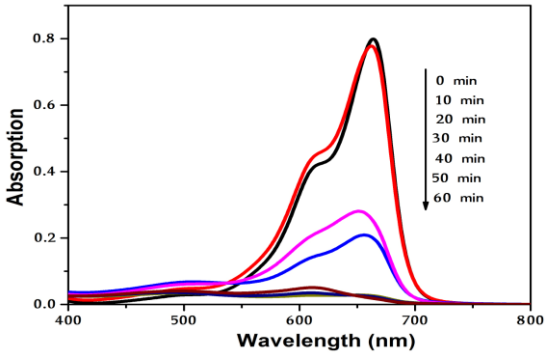

It is observed that the curve with irradiation time as abscissa and $\ln(C_t/C_0)$ as the vertical ordinate is close to a linear curve. The rate constant values (k) (Fig.10) were calculated for TiO_2, 5% Fe_3O_4@TiO_2, 10% Fe_3O_4@TiO_2 and 15% Fe_3O_4@TiO_2 as 0.0245, 0.0366, 0.0653 and 0.0457 min-1, respectively. This result indicates that the 10% Fe_3O_4@TiO_2 composite showed higher photocatalytic activity, which may be attributed to the effective charge separation of (e-…h+) pairs.

Fig.7b The time dependent absorption spectra of MB recorded in the presence of 5wt% of Fe_3O_4@TiO_2 under sunlight irradiation at different times. [Catalyst] = 1.05g/0.5L and [MB] = 1.6×10^{-5} M.

Fig.7c The time dependent absorption spectra of MB recorded in the presence of 10 wt% of Fe_3O_4@TiO_2 nanocomposite under sunlight irradiation at different times. [Catalyst] = 1.05g/0.5L and [MB] = 1.6×10^{-5} M.

Fig.7d The time dependent absorption spectra of MB recorded in the presence of 15 wt% of Fe_3O_4@TiO_2 nanocomposite under sunlight irradiation at different times. [Catalyst] = 1.05g/0.5L and [MB] = 1.6×10^{-5}

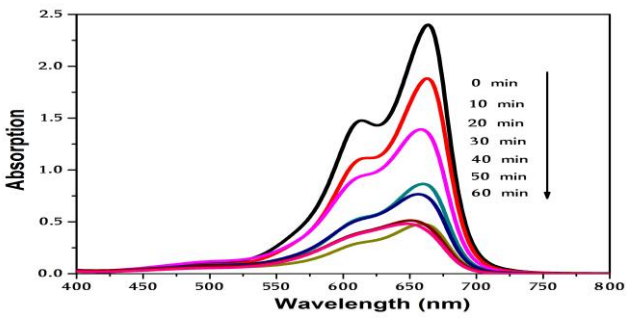

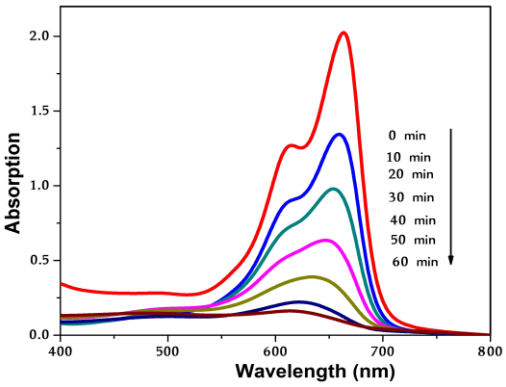

Fig.8. Photocatalytic degradation of methylene blue (MB) in the presence of different catalysts under sunlight irradiation. Bare TiO_2 (a), 5 wt% of Fe_3O_4@TiO_2 (b), 10 wt of Fe_3O_4@TiO_2 (c) and15 wt% of Fe_3O_4@TiO_2 (d). [Catalyst] = 1.05g/0.5L and [MB] = 1.6×10-5 M.

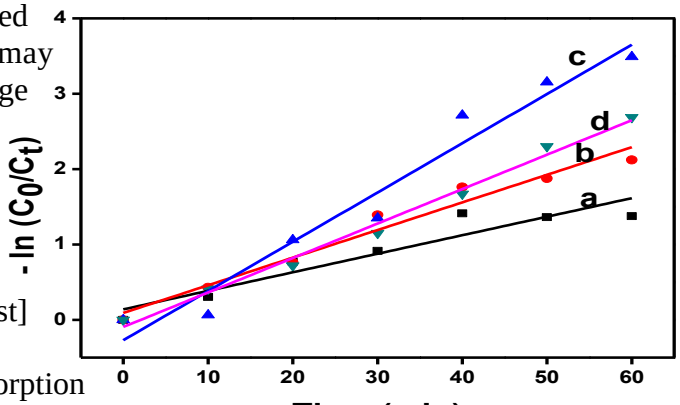

Fig.9. $\ln(C_0/C_t)$ Vs time plots for the photocatalytic degradation of MB over (a) TiO_2, (b) 5% Fe_3O_4@TiO_2, (c) 10% Fe_3O_4@TiO_2 and (d) 15% Fe_3O_4@TiO_2 core-shell nanocomposites.

Fig.10. The reaction rate constants for the photocatalytic degradation of MB over ((a) TiO_2, (b) 5% Fe_3O_4@TiO_2, (c) 10% Fe_3O_4@TiO_2 and (d) 15% Fe_3O_4@TiO_2 composites

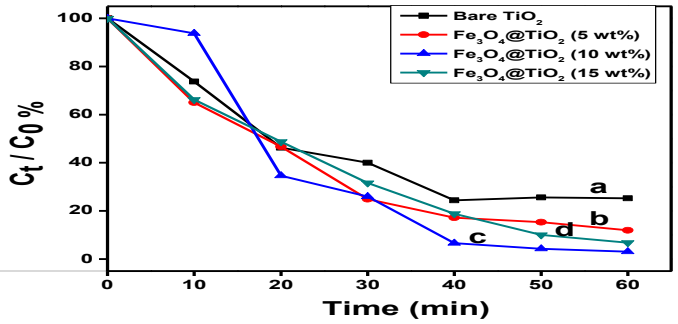

-ln (C0/Ct)

Summary & Conclusion

Fe_3O_4 doped TiO_2 nanoparticles with different doping amounts (5, 10, and 15 wt%) are successfully synthesized using co-precipitation method under otherwise identical conditions. The results indicate that the size of the TiO_2 nanoparticles decreases as the doping amount of Fe_3O_4 increases. The doping of Fe_3O_4 can control the TiO_2 crystal from anatase to rutile, broaden the width of the diffraction peaks of TiO_2, and produce a redshift in the band gap transition and an increase of absorption in visible range. It is important that an appropriate doping of Fe^{3+} (about 10wt% in our experiment) markedly improved the catalytic activity of TiO_2 under sunlight irradiation, and the catalytic activity is higher than that of the bare TiO_2. The main factors affecting the catalytic activity in these experimental conditions are concluded to be the phase and electron structures of TiO_2. It is of great significance for using solar energy as the irradiation source to improve the catalytic activity of TiO_2 obviously by appropriately doping Fe_3O_4-TiO_2. The introduction of Fe^{3+} ions in TiO_2 nanoparticles is responsible not only for reducing the photo-generated hole-electron recombination rate but also for utilizing solar energy sufficiently. Hence, it is hopeful to use Fe_3O_4 doped TiO_2 as an effective photocatalyst in the degradation of organic contaminates, cleanup of aqueous contaminates especially the aqueous contaminates of dye and so on in the fields of environmental decontamination

References

1. E. J. Weber, V. C. Stickney. Hydrolysis kinetics of Reactive Blue 19- Vinyl Sulfone, Water Res. 1993,27,63–67.

2. C. Rafols, D. Barcelo. Determination of mono- and disulphonatedazo dyes by liquid chromatography–atmospheric pressure ionization mass spectrometry, J. Chromatogr. A. 1997,777, 177–192.

3. A. Houas, H. Lachheb, M. Ksibi, E. Elaloiu, C. Guillard, J. M. Herrmann. Photocatalytic degradation pathway of methylene blue in water, Appl. Catal. B: Environ. 2001,3,145-157.

4. S. K. Kansal, N. Kaur, S. Sing. Photocatalytic degradation of commercial reactive dyes in aqueous phase using Nanophotocatalysts, Nanoscale Res. Lett. 2009, 4, 709-716.

5. A. B. Bianco-Prevot, C. Baiocchi, M. C. Brussino, E. Pramauro, P. Savarino, V. Augugliaro, G. Marcì, L. Palmisano. Photocatalytic degradation of acid blue 80 in aqueous solutions containing TiO2 suspensions. Environ. Sci. Technol. 2001, 35, 971-976.

6. L. Davydov, E. P. Reddy, P. France, P. G. Smirniotis. Sonophotocatalytic destruction of organic contaminants in aqueous systems on TiO_2 powders, Appl. Catal. B: Environ. 2001, 32, 95-105.

7. A. Fujishima and K. Honda, Electrochemical Photolysis of Water at a Semiconductor Electrode Nature, 1972, 238, 37.

8. M. Schiavello, Heterogeneous photocatalysis - Vol. 3. John Wiley & Sons, 1st Edition, 1997.

9. M. R. Hoffmann, S. T. Martin, W. Choi and D. W. Bahnemann, . Bahnemann Environmental, Applications of Semiconductor Photocatalysis Chem. Rev, 1995, 95, 69.

10. D. S. Bhatkhande, V. G. Pangarkar and A. ACM Beenackers, Photocatalytic degradation for environmental applications J. Chem. Technol. Biotechnol., 2001, 77, 102.

11. R. Abe, J. Photochem. . Recent progress on photocatalytic and photoelectrochemical water splitting under visible light irradiation Photobiol. C: Photochem. Rev., 2010, 11, 4, 179.

12. M. Kitano and M. Hara, Heterogeneous photocatalytic cleavage of water J. Mater. Chem., 2010, 20, 627.

14. X. Chen and S. S. Mao, Titanium dioxide nanomaterials: synthesis, properties, modifications, and applications,"Chem. Rev., 2007, 107, 2891–2959..

15. H. M. Sung-Suh, J. R. Choi, H. J. Hah, S. M. Koo and Y. C. Bae, , Comparison of Ag deposition effects on the photocatalytic activity of nanoparticulate TiO_2 under visible and UV light irradiation J.Photochem. Photobiol., A, 2004, 163, 37–44.

16. M. Andersson, H. Birkedal, N. R. Franklin, T. Ostomel, S. Boettcher,

A. E. C. Palmqvist and G. D. Stucky, Ag/AgCl-loaded ordered mesoporous anatase for photocatalysis Chem. Mater., 2005, 17, 1409–1415.

17. M. R. Elahifard, S. Rahimnejad, S. Haghighi and M. R. Gholami, Apatite-coated $Ag/AgBr/TiO_2$ visible-light photocatalyst fordestruction of bacteria, J.Am. Chem. Soc., 2007, 129, 9552–9553.

18. Y. Li, H. Zhang, Z. Guo, J. Han, X. Zhao, Q. Zhao and S.-J. Kim, Highly efficient visiblelight-induced photocatalytic activity of nanostructured AgI/TiO_2 photocatalystLangmuir, 2008, 24, 8351–8357.

19. K. Awazu, M. Fujimaki, C. Rockstuhl, J. Tominaga, H. Murakami,Y. Ohki, N. Yoshida and T. Watanabe, Plasmonic Photocatalyst Consisting of Silver Nanoparticles Embedded in Titanium J. Am. Chem. Soc., 2008, 130, 1676–1680

22. H. choi, M.G. Antoniou, M. Pelaez, A.A.D.L Cruz, J.A. Shoemaker and D.D. Dionysiou, Mesoporous nitrogen-doped TiO_2 for the photocatalytic destruction of the cyanobacterial toxin microcystin-lr under visible light irradiation, Environ. Sci. Technol., 2007, **41**, 7530–7535.

23. X. Wang and R.A. Caruso, Enhancing photocatalytic activity of titania materials by using porous structures and the addition of gold nanoparticles, J. Mater. Chem., 2011, **21**, 20–28.

24. M. Srinivasan and T. White, Degradation of methylene blue by three-dimensionally ordered macroporoustitania, Environ. Sci.Technol. 2007, **41**, 4405–4409.

25. J. H. Pan, H. Q. Dou, Z. G. Xiong, C. Xu, J. Z. Ma and X. S. Zhao, Porous photocatalysts for advanced water purifications, J. Mater. Chem., 2010, **20**, 4512–4528.

26. M. Li, M. K. H. Leung, D. Y. C Leung, K. Sumathy. A review and recent developments in photocatalytic water-splitting using TiO_2 for hydrogen production.A review and recent developments in photocatalytic water-splitting using TiO_2 for hydrogen production. Renew Sustain Energy Rev 2007, 11, 401-25.

27. N. Pugazhenthirana, S. Murugesana, S. Anandan, High surface area $Ag\text{-}TiO_2$ nanotubes for solar/visible-light photocatalytic degradation of ceftiofur sodium, Journal of Hazardous Materials. 2013, 263, 541– 549.

28. David, H.; Gracias, J. T.; Tricia, L. B.; Carey, H.; George, Forming Electrical

Networks inThree Dimensions by Self-Assembly M. W. Science 2000, 289, 1170–1172.

29. Guardia, P.; Labarta, A.; Batlle, X. J. Phys. Chem. C 2011, 115, 390–396.

30. Q. Li, H. Li, V. G. Pol, I. Bruckental, Y. Koltypin, J. Calderon- Moreno, I. Nowike, Gedanken, Sonochemical synthesis, structural and magnetic properties ofair-stable Fe/Co alloy nanoparticles A. New J. Chem. 2003, 27, 1194–1199.

31. X. Chen, K. M. Unruh, C. Ni, B. Ali, Z. Sun, Q. Lu, J. Deitzel, J. Q. Xiao,. Fabrication, Formation Mechanism, and Magnetic Properties of Metal Oxide Nanotubes via Electrospinning and Thermal Treatment J. Phys. Chem. C 2011, 115, 373–378.

32. C. Y. Li, Y. Lin, S. P. J Tsai, C. T Chen,W. Y Chen, Y. C. Chen, nitrilotriacetic acid-coated magnetic nanoparticles as affinity probes for enrichment of histidine tagged proteins and phosphorylated peptides Anal. Chem. 2007, 79, 7519–7525.

(33) J.Chen, L. Xu, W.Li, Gou, Fe_2O_3 nanotubes in gas sensor and lithium ion battery applications X. Adv. Mater. 2005, 17, 582–586.

(34) N.A Frey, S.Peng,K.Cheng, S.Sun, Magnetic nanoparticles: Synthesis, functionalization, and applications in bioimaging and magnetic energy storage Chem. Commun. 2009, 38, 2532–2542.

(39) L.Gao, J.Zhuang, J.Leng, J.Zhang, Y.Zhang, N.Gu, T. Wang, J. Feng, D.Yang, S.Perrett, X. Yan, Intrinsic peroxidase-like activity of ferromagnetic nanoparticles. Nat. Nanotechnol. 2007, 2, 577–583.

(40) J. M. Perez, Nat. Iron oxide nanoparticles - Hidden talentNanotechnol. 2007, 2, 535-536.

(41) T.Zeng, W. W. Chen, C. M Cirtiu, A. Moores, G. Song, C. Li, Fe3O4 nanoparticles: robust and magnetically recoverable catalyst for three-component coupling of aldehyde, alkyne and amine J. Green Chem. 2010, 12, 570–573.

42 G. Sun, B. Dong, M. Cao,.; B. Wei, Hu, Hierarchical dendrite-like magnetic materials of Fe_3O_4, γ-Fe_2O_3, and Fe with high performance of microwave absorption C. Chem. Mater. 2011, 23, 1587–1593.

(43) D. W. Elliott, W. X. Zhang, Field assessment of nanoscale bimetallic particles for groundwater treatment. Environ. Sci. Technol. 2001, 35, 4922–4926.

(44) M. Takafuji, S.Ide, H.Ihara, Xu, Preparation of Poly(1-vinylimidazole)-Grafted Magnetic Nanoparticles and Their Application for Removal of Metal Ions Z. Chem. Mater. 2004, 16, 1977–1983.

(45) T. Arai, T. Sato, H. Kanoh, K. Kaneko, K. Oguma, A.Yanagisawa, Chem.sEur. J. 2008, 14, 882.

(46) H.Yoon, S. Ko, Jang, Nitrogen-doped magnetic carbon nanoparticles as catalyst supports for efficient recovery and recycling J. Chem. Commun. 2007, 1468–1470.

(47) D. K .Yi, S. S. Lee, J. Y. Ying, Chem. Mater. 2007, 18, 2459.

(48) M. Shokouhimehr, Y.Z. Piao, J. Y. Kim, Y. J. Jang, T. W. Hyeon, Angew. magnetically recyclable nanocomposite catalyst for olefin epoxidation Chem., Int. Ed. 2007, 46, 7039.

(49) D.Beydoun, R. Amal, G. K. C. Low, Mcevoy, novel photocatalyst titania coated magnitite activity and photodissolution S. J. Phys. Chem. B 2000, 104, 4387.

(50) B. P. Zhang, J. L Zhang, F. Res. Chen, Magnetically Separable Fe_3O_4/TiO_2 Hollow Spheres: Fabrication and Photocatalytic Activity, Chem. Int. 2008, 34, 375.

(51) S. W Lee, J.Drwiega, C. Y. Wu, D.Mazyck, W. M. Sigmund, Chem. Anatase TiO_2 nanoparticle coating on barium ferrite using titanium bis-ammonium lactato dihydroxide and its use as a magnetic photocatalys. Mater. 2004, 16, 1160.

(52) T. A Gad-Allah, S. Kato, S. Satokawa, Kojima, roll of core diameter and silica content in photocatalytic activity of $TiO_2/Sio_2/Fe_3O_4$ composite T. Solid State Science 2007, 9, 737.

53. S. S. Rayalu, D. Jose, P. A. Mangrulkar, M. Joshi, G. Hippargi , K. Shrestha , K. Klabunde Photodeposition of AuNPs on metal oxides: Study of SPR effect and photocatalytic activity International journal of hydrogen energy 2014, 39, 3617-3624.

54. Y. Liu, L. Yu, Y. Hu, C. Guo, F. Zhanga and X. W. Lou A magnetically separable photocatalyst based on nest-like g-Fe_2O_3/ZnO double-shelled hollow structures with enhanced photocatalytic activity Nanoscale (RSC), 2012, 4, 183-187.

55. M. Zhu and G. Diao, Synthesis of porous Fe_3O_4 nanospheres and its application for the Catalytic degradation of xylenol orange, Journal of physical chemistry C, 2011, 115, 18923–18934.

56. R. Chalasani and S. Vasudevan, cyclodextrin-functionalized $Fe_3O_4@TiO_2$: reusable, magnetic nanoparticles for photocatalytic degradation of endocrine-disrupting chemicals in water supplies, 2013, 7, 4093–4104.

57. Y. Lin, Z. Geng, H. Cai, Lu Ma, J. Chen, J. Zeng, N. Pan, and X. Wang Ternary Graphene TiO_2–Fe_3O_4 Nanocomposite as a Recollectable Photocatalyst with Enhanced Durability Eur. Journal of Inorganic Chemistry. 2012, 4439 –4444.

58. Z. Ali1, S. T. Hussain, M. N. Chaudhry, S. A. Batool, and T. Mahmood Novel nano photocatalyst for the degradation of sky blue 5b textile dye International journal of physical sciences , 2013. 8, 1201-1208.

59. S. Xuan, W. Jiang, X. Gong, Y. Hu, and Z. Chen, Magnetically Separable Fe_3O_4/TiO_2 Hollow Spheres: Fabrication and Photocatalytic Activity, Journal of physical chemistry. C 2009, 113, 553–558.

60. L. RuiHua, H. Jiang, H. LiZhen, G. Xia, D. X. Yan and Z. Jie, Synthesis and characterization of bifunctional terbium complex-based nanoparticles, chines science bulletin, 2012, 57, 750-755.

61. A. Hasanpour, M. Niyaifar, H. Mohammadpour, J. Amighian, A novelnon-thermal process of TiO_2-shell coatingon Fe_3O_4-core nanoparticles, Journal of Physics and Chemistry of Solids 2012, 73, 1066–1070.

62. Y. Hu, Y. Liu, H. Qian, Z. Li and J. Chen, “Coating colloidal carbon spheres with CdS nanoparticles: microwave-assisted synthesis and enhanced photocatalytic activity,”Langmuir, 2010, 26, 18570

63. H. F. Jin, W. G. Li, J. M. Xiang, J. Y. Nanometer particle of Fe^{3+}/ TiO_2/ SiO_2 complex: synthesis and usefulness in photocatalytic degradation of nitrite. Chinese journal of Applied chemistry, 2001, 18, 636-639.

64. S. Xuan, W. Jiang, X. Gong, Y. Hu, and Z. Chen, Magnetically Separable Fe_3O_4/TiO_2 Hollow Spheres: Fabrication and Photocatalytic Activity, Journal of Physical Chemistry. C 2009, 113, 553–558.

65. P. F. Yan, F. Q. Wu, X. Jiang, D. R. Zhou. H. G. Fu preparation and catalytic properties of iron-doped TiO_2 nanocrystal, Material Science and technology, 2002, 10, 28-31.

66. W.Gao, F.Q.Wu, Z. Luo, J.X. Fu, Wang D J, Xu B K. Studies onthe relationship between the crystal form of TiO_2 and its photocatalyzing degradation efficiency. Chemical Research In Chinese Universities, 2001, 22: 660–662.

67. W Y. Choi, A. Termin, M R. Hoffmann. The role of metal ion dopantsin quantum-sized TiO_2: Correlation between photoreactivity and charge carrier recombination dynamics. Journal of Physical Chemistry, 1994, 98: 13,669–13,679.

68. A L. Linsebigler, G. Lu and J T. Yates Photocatalysis on TiO2 Surfaces: Principles, Mechanisms, and Selected Results Chem. Rev. 1995,95, 735

69. X. Chen and S S. Mao "Titanium Dioxide Nanomaterials: Synthesis, Properties,
Modifications and Applications" Chemical Review. 2007,107, 2891

70. B. Subash, B. Krishnakumar, V. Pandiyan, M. Swaminathan and M. Shanthi, An efficient nanostructured Ag_2S–ZnO for degradation of Acid Black 1 dye under day light illumination, Sep. Purif. Technol., 96 , 204–213.